



ELSEVIER

Contents lists available at SciVerse ScienceDirect

Acta Astronautica

journal homepage: www.elsevier.com/locate/actaastro

Electrostatically inflated gossamer space structure voltage requirements due to orbital perturbations



Laura A. Stiles^{a,*}, Hanspeter Schaub^a, Kurt K. Maute^a, Daniel F. Moorer^b

^a Aerospace Engineering Sciences Department, University of Colorado, Boulder, CO, United States

^b Wacari Group LLC, Boulder 80301, United States

ARTICLE INFO

Article history:

Received 10 April 2012

Received in revised form

12 November 2012

Accepted 17 November 2012

Available online 10 December 2012

Keywords:

Electrostatic inflation

Gossamer spacecraft

Inflatable structures

ABSTRACT

This paper explores the concept of using electrostatic forces for deployment of gossamer space structures. The Electrostatically Inflated Membrane Structure (EIMS) uses two conducting membranes that are interconnected through membrane ribs. An absolute electrostatic charge is applied to the structure through active charge emission. This causes repulsion between layers of lightweight membranes that inflates the EIMS system and tensions the membranes. Assuming positive tensions, the EIMS system is modeled as a rigid system. Typical orbital perturbations are considered such as solar radiation pressure, differential gravity, and atmospheric drag which may compress the structure leading to shape destabilization. Restricting the analysis in this paper to flat membranes, the minimum potentials required to exactly compensate for the worst case scenario of differential solar radiation pressure at geostationary altitudes are estimated to be on the order of hundreds of volts. In low Earth orbit, voltage magnitudes of several kilovolts are required to reach an inflation pressure to offset the normal compressive drag pressure.

© 2012 IAA. Published by Elsevier Ltd. All rights reserved.

1. Introduction

Lightweight, gossamer spacecraft structures provide an interesting alternative to the traditional mechanical systems that are typically more massive and expensive to launch. Many different applications of gossamer space hardware have been explored, and a select few have been successfully employed in space. Examples of early work on inflatable structures include the development of the Mylar ECHO balloons in 1958 at NASA. The ECHO I sphere, which was launched in 1960, successfully served as a communications reflector in space for several months [1]. L'Garde Inc. made early contributions to the field of deployable technology, including the support for NASA to launch an inflatable antenna from the Space Shuttle [2]. Examples of present day gossamer spacecraft research

include solar sail technology [3], inflatable solar arrays [4], and space habitats [5].

Common methods for deployment of gossamer structures include inflation via pressurized gas, sublimating chemicals, or evaporating liquids [6]. This paper explores a novel inflation method of a membrane space structure, which uses electrostatic repulsion to create inflationary forces [7,8]. Applying absolute electric charge to a layered gossamer structure provides an inflationary pressure due to the repulsive electrostatic forces between the charged layers, as per Coulomb's law. The electrostatic pressure inflates the membranes to a stable structure, much like inflation of an airbag with gas. The separation distance due to inflation of the membranes is constrained by an internal membrane structure. However, in contrast to gas-inflated structures, the electrostatically inflated structure does not suffer from sensitivities to membrane punctures or the requirement to be a closed structure. In fact, the simple concepts considered in this paper are open ended membrane structures resembling more the ribbed open

* Corresponding author.

E-mail address: lastiles@gmail.com (L.A. Stiles).

Nomenclature

A	area, m^2
C	capacitance, F
d	separation distance, m
E	electrostatic field, N/C
$F_{disturb}$	disturbance force, N
F_D	drag force, N
F_e	electrostatic force, N
F_g	gravitational force, N
m	mass, kg
n	number density, m^{-3}
P_D	drag pressure, N/m^2
P_g	gravitational pressure, N/m^2
P_{SRP}	solar radiation pressure, N/m^2

Q	charge, C
r	radial distance, m
t	thickness, m
T_e	electron temperature, K
T_i	ion temperature, K
F_R	rib tension, N/m^2
v	velocity, m/s
V	voltage, V
x_1	distance to membrane 1, m
x_2	distance to membrane 2, m
λ_D	Debye length, m
ρ	density, kg/m^3
σ	charge density, C/m^2
ϕ	electric potential, V

structure of a ram-air parachute than that of a fully enclosed balloon. The electrostatic inflation idea is illustrated in Fig. 1.

The electrostatic inflation concept is particularly applicable to structures such as arrays, solar power reflectors, or drag augmentation devices for de-orbiting and space debris avoidance purposes. Further, Tripathi discusses in Ref. [9] using large, charged space structures to perform active radiation shielding to protect humans during space flight. The EIMS concept would enable novel structural solutions where charging is used both for active radiation shielding as well as providing lightweight membrane structure shape stability. In applying electrostatics for inflation of these and other space apertures, there is the potential to significantly decrease overall mass, while reducing the associated deployment-oriented power and packing volume for large, lightweight deployable structures. A large ratio of deployed volume to stowed volume is very advantageous, especially in highly volume-constrained spacecraft such as Nanosats or CubeSats.

In this paper, the prospects and challenges of the EIMS concept are explored. Restricting our analysis to the case of two flat parallel membranes, the membrane-normal orbital perturbations to the system are evaluated. The goal is to understand the magnitude of external orbital forces and pressures which attempt to compress a membrane structure and a resulting deflation of the system. Note, lateral shearing perturbations are beyond the scope of this study and will be addressed in future work. The shearing resistance is strongly dependent on the choice of the particular internal membrane structure. Rather, this paper focuses on what orbital perturbations will cause membrane-normal deflation, and what minimum voltages are required to compensate. Based on the orbital perturbations considered, minimum membrane required charge densities are determined to exactly counter the compressive perturbations and maintain inflation. Next the challenging question as to what potential, not charge density, is required to compensate for orbital perturbations is addressed, including a study of geometric configuration

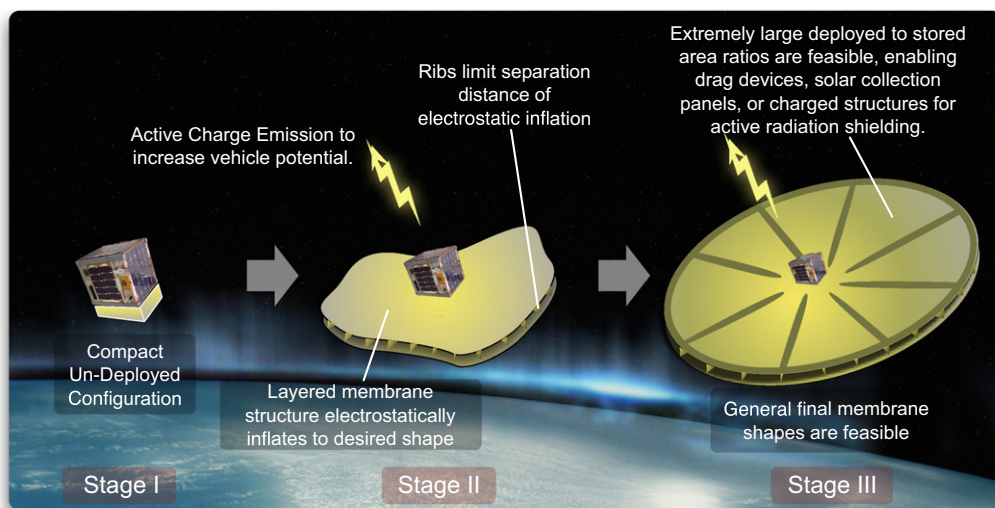


Fig. 1. Illustration of electrostatically inflated membrane structure (EIMS) concept.

effects on the capacitance of the system. Numerical finite element simulations are employed to study the full electrostatic response and compare to the simplified analytical predictions.

2. Background

The concept of electrostatics for control of space structures has been studied for many decades. The previous research has mainly focused on using electrostatics to precisely control the shape of single-layer membrane surfaces whose outer edges are held in place by a rigid structure. A US patent by J.H. Cover filed in 1966 describes an invention for using electrostatics to control the surface of a reflector dish in space [10]. This patent also discusses how electrostatic forces can be created using active charge emission using only Watt levels of power at geosynchronous orbit altitudes. However, the electrostatics are only used to shape a single membrane. In contrast, the EIMS concept presented in this paper uses electrostatics to inflate a layered membrane structure which does not require a rigid outer structure. Electrostatically controlling the surface of membrane mirrors in space has also been studied, such as the work of Errico et al. in Ref. [11]. Again, these designs significantly differ from the proposed membrane structure inflation as the mirror and reflector technology requires a rigid external structure to support the surfaces. With EIMS, the gossamer structure is completely and compactly stowed until the charge level is increased to cause the entire structure to inflate.

Another field of related research is Coulomb control for free-flying spacecraft. This application aims to raise the absolute potential of the spacecraft to control the electrostatic interactions with surrounding vehicles. Actively charging a craft to a few kilovolts causes electrostatic forces between the craft of micro- to milli-Newton levels with millisecond charging time [12,13]. In Refs. [14,15] the Coulomb forces are explored to develop static virtual structures subject to both to the gravitational and electrostatic force fields. Feedback control strategies of such virtual structures have only been developed for simple 2- and 3-craft systems thus far [16,17]. A related concept to the proposed electrostatic membrane structure is the Tethered Coulomb Structure (TCS) [18,19]. Here the complex charged relative orbital motion is constrained through the use of tethers of sub-millimeter level thickness interconnecting the charged nodes. The electrostatic force is used to create an inflationary pressure to ensure positive tether tension at all times. Thus, the TCS can essentially be considered as a larger scale, discrete element precursor of EIMS. EIMS differential orbital perturbations that drive charging requirements are different than those of a TCS due to the larger mass and separation distances of the TCS system (50–100 kg nodes and multiple meters), versus the sub-kilogram membrane structure mass and centimeter separation considered for EIMS.

The challenge of controlling the potential of a body in space has been successfully flight tested. The SCATHA (Spacecraft Charging at High Altitudes) experiment was one of the spaceflight experiments that demonstrated use

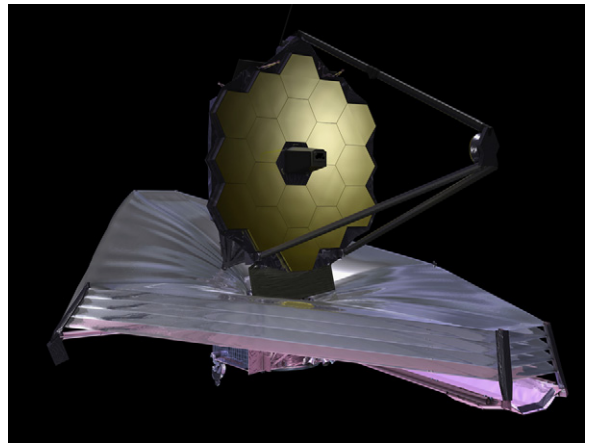


Fig. 2. James Webb Space Telescope.

of ion and electron guns to control spacecraft surface potential to 10–20 kV [20,21]. Even without active charging, spacecraft can charge up to many kilovolts in the plasma environment. The highest recorded natural charging event occurred on the ATS-6 spacecraft, reaching a potential of -19 kV during an eclipse period of the GEO orbit [22]. While the previous two examples are space missions with active charge control at geosynchronous altitudes, the SPEAR I mission is an example of a charging experiment at Low Earth Orbit (LEO). The SPEAR I mission employed active charging of test spheres in LEO with an altitude of approximately 350 km [23]. Using a capacitor, a positive potential of 45.3 kV was applied to two 10 cm radius spheres attached to a rocket body [23]. The current CLUSTER mission also employs active charge control through continuous charge emission to serve the spacecraft absolute potential to a desired near-zero charge level. The charge control of a spacecraft is, however, complicated by the presence of the plasma environment. While at geostationary altitudes the charge control can be achieved with low electrical power levels [10,24], the relatively cold and dense plasma at low Earth orbits makes charge control more challenging. LEO applications would require more power, and the electrostatic field about a charged body is more quickly negated by the surrounding plasma charge. This and other challenges for EIMS are further discussed in the next section.

3. Prospects and challenges of electrostatic inflation

3.1. EIMS concept discussion

The concept of electrostatic inflation is applicable for gossamer structures on spacecraft. To illustrate the concept, the James Webb Space Telescope shown in Fig. 2 is used as an example.¹ The telescope has a large sunshield consisting of several layers of silicon-coated Kapton which is used to reflect the heat of the sun, keeping the telescope cool. The layers of Kapton are mechanically

¹ www.jwst.nasa.gov/images.

tensioned to maintain the desired shape. The electrostatic inflation concept is envisioned to support a similar layered structure, yet without the external tensioning system. The pressure to maintain shape is provided by repulsive forces between electrostatically charged layers. Before changing the electrostatic potential of the structure, there is no stiffness to the body to maintain a desired shape. When the absolute potential has been raised, the electrostatic charge distributed across a layered structure results in electrostatic forces acting between the layers of the conducting material. These forces act as inflation pressure, similar to gas inflation. Like a ram-air parachute, the layered structures are envisioned to have ribs between the layers to tension the structure as illustrated in Fig. 3.

For the modeling purposes of this paper, the lightweight membrane ribs are assumed to only be able to provide tensile forces between the layers of the structure. The investigation of required electrostatic charge or potential for inflation presented in this paper is limited to 2-layer gossamer structures in this sandwich-like configuration. This study makes the simplifying assumption that the outer membranes are flat and rigid, and therefore ignore displacement effects such as geometric

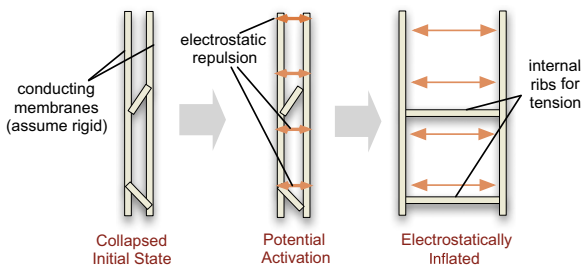


Fig. 3. Simplified open-ended membrane rib structure undergoing electrostatic inflation.

stiffening and interactions between deforming structure and electrostatic forcing. Future work will investigate the bulging effects that can occur between the rib-membrane attachment points. Additionally, it is assumed that there is no rotation of the structure. Rotation will introduce additional shearing pressures on the membranes. This shearing can be partially negated by the rib structure. However, such detailed EIMS modeling is beyond the scope of this paper. Rather, the presented work focuses on disturbances that can cause an EIMS surface normal compression, and investigates what potentials are required to compensate.

Fig. 4 shows force diagrams of the disturbance pressures and forces acting on EIMS for the cases of a disturbance acting on a single membrane (solar radiation or drag) and a disturbance pressure which compresses both membranes simultaneously (differential gravity). The solar radiation pressure and drag pressure are assumed to be in a worst-case alignment that causes compression of the membrane structure. The internal rib structure is shown as holding the system in tension as the electrostatic pressure causes inflation between the membranes. For the analysis in this paper, failure of the structure is defined as compression of the two membranes from disturbance pressures and violating the rigid body assumption. Nominally the internal inflationary forces are larger than the external disturbance forces. Here the rib forces F_R are positive and maintain a fixed separation distance d , thus keeping EIMS rigid. Unless the external disturbance forces are large enough to cause the rib tensions to be negative (compressive), EIMS maintains a fixed shape as it translates due to a net external disturbance. Of interest is what minimum electrostatic potentials are required to compensate for the membrane-normal orbital disturbance such that separation distance remains constant.

This study investigates the impact of these disturbing orbital pressures acting normal on the EIMS surface

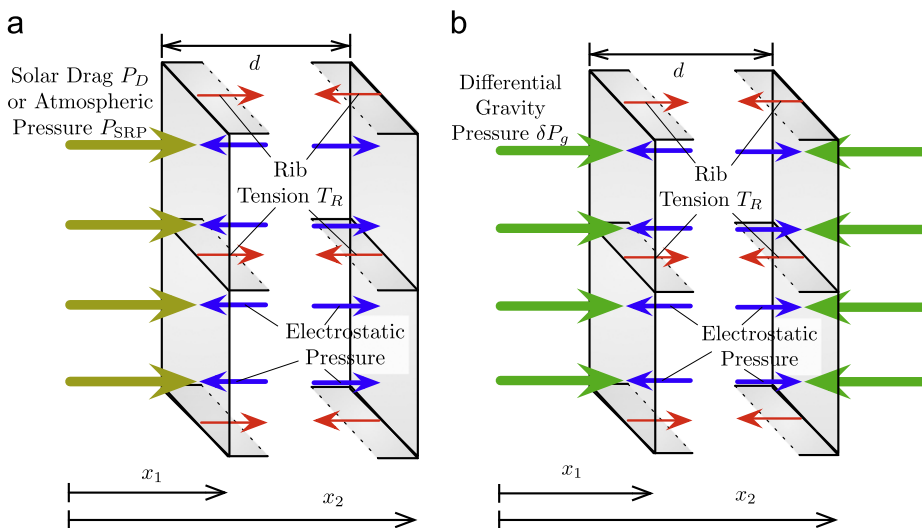


Fig. 4. Force diagrams of the EIMS membrane-normal pressures and forces. (a) Solar radiation and atmospheric drag pressure acting on a single membrane causing an inertially accelerating EIMS system and (b) Differential gravity configuration compressing both membrane surfaces with EIMS inertially fixed.

(causing deflation) using the following simplified model of an electrostatically inflated membrane structure. The relationship between the minimum required electrostatic inflation pressure and the orbital perturbations is studied by examining the dynamics of the two membrane system shown in Fig. 4. For a system with disturbance pressures acting on one membrane only (i.e. solar or atmospheric drag), the equations of motion for membrane 1 and membrane 2 are:

$$m\ddot{x}_1 = F_{\text{disturb},1} - F_e + F_R \quad (1a)$$

$$m\ddot{x}_2 = m(\ddot{x}_1 - \ddot{d}) = m\ddot{x}_1 = F_e - F_R \quad (1b)$$

where m is the membrane mass, F_e is the electrostatic force, F_R is the rib force, and $F_{\text{disturb},1}$ is the one-sided disturbance force. These simplified equations are a good approximation of the first-order EIMS compression dynamics as EIMS is assumed to not be rotating in this structure. Further, these equations are also suitable for an EIMS in Earth orbit if the structure is assumed to not be rotating relative to the local-vertical, local-horizontal (LVLH) frame. In this normally static orientation case the orbital Coriolis terms have no impact on the compression dynamics. If the structure does not deform due to the external disturbance, the separation distance, d , remains constant. Also, the rib force, F_R will be zero in the case of minimum electrostatic pressure. Substituting Eqs. (1a) into (1b) yields the relationship:

$$F_e = \frac{F_{\text{disturb},1}}{2} \quad (2)$$

Because the one-sided disturbance is causing EIMS to accelerate, the electrostatic inflation force must be half of the disturbance force. The previous scenario applies for solar radiation and atmospheric drag disturbances. For differential gravity disturbances, however, the disturbance pressure acts on both membranes. By the same approach, the required electrostatic for relationship for this scenario is found to be:

$$F_e = F_{\text{disturb},2} \quad (3)$$

This relationship between the forces will be used to later determine the minimum required charge densities and voltages to maintain a constant separation between membranes under the compressive pressures of worst-case orbital perturbations.

Many other challenges to electrostatic inflation exist such as membrane wrinkling, thermal stresses in the membranes, orbital perturbations, complex electrostatic fields, plasma Debye shielding and the time varying space plasma environment. In the plasma environment of space, electrons and ions rearrange in the presence of a disturbing electric field to maintain macroscopic neutrality [25]. This phenomena, known as Debye shielding, will effectively shield the electrostatic potential of a charged object in a plasma, such as an electrostatically inflated structure. In the Low Earth Orbit region, Debye lengths are typically on the order of milli- or centimeters, depending on the orbit altitude. If the separation distance between the layers of membrane in a gossamer structure in LEO is greater than a few centimeters, or on the order of the local Debye length, then the membranes may not experience a

significant electrostatic force and the inflation concept would not be feasible. The details of the LEO plasma flows about an EIMS concept with strong Debye shielding are still being investigated. However, large membrane separation distances will become increasingly challenging in this orbit regime. In the GEO regime, the Debye length is generally on the order of hundreds of meters. The small separation distances between proposed membrane structures compared to the large Debye lengths yield nearly negligible effects from the shielding, and the field decreases proportional to the $1/r^2$ vacuum electrostatic field dropoff. This is true even for the very worst GEO plasma weather conditions being considered.

There are many challenges for electrostatic inflation that are beyond the scope of this paper. One challenging issue is the storage and deployment of the structure. In laboratory tests to inflate a structure, such the one illustrated in Fig. 3, a non-conducting gap or layer between conducting surfaces is required for electrostatic inflation to occur. Without a gap, the layers of charged conducting sheets do not separate due to stickage between the tested membranes. For electrostatic inflation, it is speculated that non-connected segments are needed between the conducting surfaces such as gaps or unpolarized dielectric layers. Understanding the physical mechanism between sticking layers in atmospheric or space environments remains as future work. In laboratory inflations, a small gap with air between surfaces has been shown as sufficient for inflation to occur across a comparatively large structure. These results are discussed in the next section. The following work assumes that the two plates are already minimally separated such that electrostatic repulsion can occur. Of interest is the following: what potentials are required to be able to overcome the differential orbital perturbations experienced either at GEO or LEO altitudes which could collapse the structure.

3.2. Laboratory demonstration of electrostatic inflation

To explore the concept of electrostatic inflation and test the feasibility of the concept in a laboratory environment, laboratory demonstrations were designed for the 1-g environment. These demonstrations are not representative of space situations but serve to demonstrate feasibility of using electrostatics for inflation pressure and to better understand the possible applications of this concept. At this stage, the laboratory results are predominantly qualitative.

The setup consists of a variety of aluminized Mylar membrane structures being charged with a Van der Graaf generator or a high voltage power supply. Fig. 5 shows a ribbed 2-membrane structure resting on a conducting surface which is connected to a high voltage power source. In this 1-g test environment, the forces on the lower plate are always balanced by the normal force of the object upon which it rests. The other plate is subjected to the Coulomb force to inflate, the compressive force of gravity, and tension in the ribs to hold the structure together. This setup is much like the worst-case along-track orbit configuration in which the differential solar radiation pressure and/or the differential atmospheric



Fig. 5. Electrostatic inflation of a test sandwich structure, from 0 kV to 9 kV.

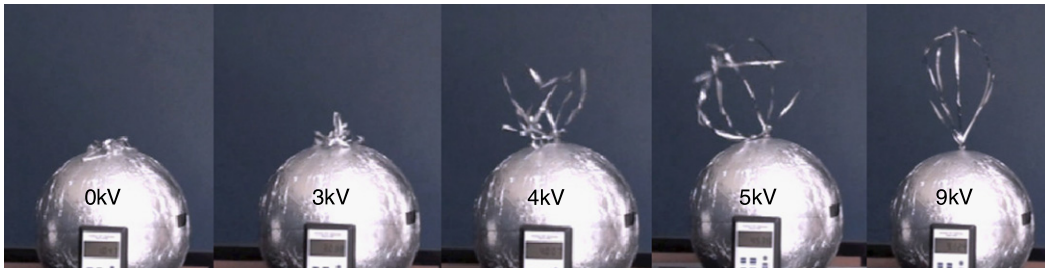


Fig. 6. Electrostatic inflation of gossamer ribbon test structure, from 0 kV to 9 kV.

drag are acting to collapse one membrane onto the other (assumed fixed) membrane. The structure used in the test shown in Fig. 5 consists of two 12×15 cm plates of 75 gauge aluminized Mylar. Three aluminized Mylar ribs connect the two membranes. Voltage was applied to the conducting sphere on which the membrane structure rested.

Video snapshots of an inflation demonstration are shown in Fig. 5 to show that in the laboratory environment, a membrane structure can transition from a collapsed initial state to an inflated state using only electrostatic pressure. Inflation occurred between 7 and 13 kV during different inflation trials. The duration of the inflation shown between the first and last frames of Fig. 5 is approximately 5 s.

Another laboratory demonstration shown in Fig. 6 shows the inflation of a gossamer ribbon structure, an example of a structure with large open surface segments. This ribbon structure was initially compacted to height of approximately 2 cm, then inflated to a height of 25 cm. This demonstration shows the potential of high deployed to stowed volume ratios with the electrostatic inflation concept. Notice in this photo series that the structure has obtained the fully inflated shape at 5 kV, yet gravity is preventing the structure from standing upright. As the voltage increases to 9 kV, the electrostatic repulsion between the ribbon structure and the conducting surface to which it is attached cause the entire structure to become upright as well as inflated to the desired shape.

As these laboratory demonstrations suffer from interactions with the atmosphere, electrostatic inflation tests were also performed in a vacuum chamber. A chamber environment of approximately 10^{-6} Torr was used to verify inflation capabilities in a vacuum. It was found that less potential was required for inflation in the vacuum environment than the atmospheric environment.

Demonstrations indicate that such self-supporting membrane structures can repeatedly and reliably be

electrostatically inflated in a laboratory environment. Such physical results are useful to explore appropriate materials, construction methods, packing methods, and charging behaviors that lead to desirable membrane motions. Further, such testing will be used in the future for validation and verification purposes of to be developed high fidelity modeling of charged membrane structures. The relatively small potential levels required to inflate the sandwich structure in 1-g are promising to the concept of electrostatic inflation for space structures. As the orbital disturbance pressures are orders of magnitude smaller than the pressure due to gravity in the 1-g environment, required potential could be much smaller than required in Earth-based experiments. It is even possible that natural charging phenomena in orbit will provide sufficient potentials for inflating gossamer structures.

4. Space weather impact

4.1. Debye shielding of point charges

In the plasma environment of space, electrons and ions rearrange in the presence of a disturbing electric field to maintain macroscopic neutrality [25]. This phenomena, known as Debye shielding, will effectively shield the electrostatic field of a charged object in a plasma, such as an electrostatically inflated structure. To determine the potential near a charged object in a plasma, the number density of charged particles must be known. An expression for the electron density and ion density are given in Eqs. (4) [25], where k is the Boltzmann constant, T is temperature, ϕ is the potential due to a charge, and n_0 is a constant particle density where $n_e(\infty) = n_i(\infty) = n_0$.

$$n_e = n_0 e^{e\phi/kT_e} \quad (4a)$$

$$n_i = n_0 e^{-e\phi/kT_i} \quad (4b)$$

Using these definitions for particle number densities, the electrostatic potential is given by Gauss's law:

$$\nabla^2 \phi = -\frac{\rho}{\epsilon_0} = \frac{n_0 e}{\epsilon_0} (e^{-e\phi/kT} - e^{e\phi/kT}) \quad (5)$$

This classical development continues under the assumption that the potential energy of the field is much smaller than the kinetic energy of the particles, or ($e\phi \ll kT$). This assumption yields the simplified expression:

$$\nabla^2 \phi = \frac{2}{\lambda_D} \phi \quad (6)$$

where the parameter, λ_D is the Debye Length. The Debye length describes the distance at which a charge is essentially shielded by the plasma if ($e\phi \ll kT$) is true. The Debye length is determined by plasma conditions through

$$\lambda_D = \left(\frac{\epsilon_0 kT}{n_e e^2} \right)^{1/2} \quad (7)$$

where e is the elementary charge. This particular form of the Debye length computation assumes that the negative plasma electrons dominate the electrostatic charge shielding. The simplified form of Poisson's equation has a well known analytical solution for the potential surrounding a point charge, q_1 , (or a charged sphere with total charge q_1) in spherical coordinates given by:

$$\phi = \frac{k_c q}{r} e^{-r/\lambda_D} \quad (8)$$

The Debye shielded electrostatic force experienced by a 2nd point charge q_2 is derived by taking the gradient of Eq. (8):

$$F = \nabla \phi \cdot q = \frac{k_c q_1 q_2}{r^2} e^{-r/\lambda_D} \left[1 + \frac{r}{\lambda_D} \right] \quad (9)$$

While this force computation is only valid for point charges, and not the flat membrane models considered in this paper, Eq. (9) provides insight into how the plasma Debye length can limit the electrostatic actuation. No simple analytical expression describes the electrostatic force between two plates, therefore numerical simulations of plasma conditions will be required for these more complicated geometries.

It should be noted that the force is a function of the gradient of the potential. Therefore if there is a steep gradient in potential due to aggressive Debye shielding, the electrostatic force can actually be larger than the vacuum force. Also, it should be noted that this equation development assumes that ($e\phi \ll kT$). If this condition is violated, the Debye length can be significantly larger. These increased effective Debye lengths are discussed further in Refs. [7,26]. The required voltage calculations in this paper, however, consider conditions under which the Debye shielding can be treated as negligible in regard to the electrostatic force computation. This can be achieved through either flying the electrostatically inflated membrane structures at particular orbit altitudes or employing large potentials.

4.2. Orbit regions applicable for electrostatic inflation

Debye shielding has a large impact on the use of electrostatics in a plasma environment. In the Low Earth Orbit region, Debye lengths are typically on the order of

Table 1
Range of feasible plasma Debye lengths.

	Smallest λ_D (m)	Nominal λ_D (m)	Largest λ_D (m)
LEO environment	0.002	0.005	0.013
GEO environment	4	200	743

milli- or centimeters, depending on the orbit altitude. Table 1 shows the extremes of Debye lengths experienced in LEO at an orbit altitude of approximately 350 km, as predicted by the International Reference Ionosphere model and reported in Ref. [27].

In earlier work on Coulomb control of free-flying charged spacecraft, or the electrostatic inflation of TCS concepts over several meters, this aggressive Debye shielding prevented such concepts from being considered at LEO [13,28]. However, with the electrostatically inflated membrane structures, even with surface areas of multiple square meters, the electrostatic force only has to occur across the membrane gap layer separation distance d which can be on the order of centimeters. If the separation distance between the membrane layers of a sandwich structure in LEO is greater than a few millimeters or centimeters, or of the order of the local Debye length, then the membranes would not experience a significant electrostatic force and the inflation concept would not be feasible. This argument assumes that the membrane potential ϕ satisfies the condition that ($e\phi \ll kT$). It has been shown that high potentials which violate this condition yield reduced Debye shielding effects, with LEO Debye Lengths raised to several decimeters [29]. Thus, if small membrane gaps, d , of less than a centimeter are assumed, then even with the aggressive Debye shielding assumptions electrostatic inflation is still feasible at LEO.

Dissimilar to earlier work on free-flying charged spacecraft where the formation size is directly limited by the electrostatic force drop off with separation distance, the membrane structure can scale to comparatively large dimensions. With EIMS, it is not necessary for the electrostatic repulsion to occur across the entire membrane surface with width w and length l dimensions of meters, only across the much smaller separation distance d with dimensions of centimeters.

In the GEO regime, the Debye length is generally on the order of hundreds of meters. However, these values vary drastically with the solar storm activities heating up part of the plasma sheath, or pushing the lower and colder plasma pause conditions into the GEO altitudes [30,31]. The upper and lower bounds of possible geostationary Debye length values are shown in Table 1, as well as the nominal value. These Debye lengths are based on observations from the ATS-5 and ATS-6 spacecraft given in Refs. [32,33]. The small separation distances between proposed membrane structures compared to the comparatively large Debye lengths yield nearly negligible effects from the shielding. This is true even for the very worst GEO plasma weather conditions being considered.

The LEO Debye lengths [34] illustrate that electrostatic inflation will require small membrane separation distances. However, because the potentials (kilovolts) are large in comparison to the cold LEO plasma temperatures, the effective Debye lengths are multiple times larger. These values do not indicate that EIMS is feasible at LEO, but it can be considered if a compatible set of potentials and separation distances are used.

5. Orbit perturbations affecting electrostatic inflation

5.1. GEO orbit perturbations

For electrostatic inflation, potentials must be high enough to produce sufficient electrostatic inflation pressure in the normal direction for self-repulsion to offset the normal compressive differential pressures from gravity, solar radiation pressure, and drag that would be experienced in orbit. Failure of the system occurs when the compressive pressures become greater than the inflation pressure, thus collapsing or deflating the structure. The worst case scenario is studied to understand the largest orbit disturbance magnitudes that may be experienced. These perturbations are assumed to be distributed over the membrane surface in the normal direction and the strong assumption of flat membranes (no bulging between the ribs) is made. In the GEO environment, atmospheric drag is not a consideration, but differential gravity and solar radiation pressure are investigated. The effect of differential gravity depends on the orbit configuration as this perturbation will tension the structure in the membrane-normal direction in the radial configuration, compress the structure in the orbit normal configuration, and have no effect in the along-track configuration.

The linearized differential gravity in the orbit radial configuration shown in Fig. 7(a) is given by Eq. (10) where μ is the gravitation parameter, r_c is the radius from Earth, and d is the separation distance of the membrane plates [28]. In this configuration the differential gravity force will aid in tensioning the structure, as the plate nearest to Earth will experience a stronger force due to gravity.

$$\delta F_{g,\text{radial}} \approx m \frac{3\mu}{r_c^3} d \quad (10)$$

For this study, mass is estimated from density, ρ and approximate material volume with area, A , and thickness, t

$$m = \rho A t \quad (11)$$

75 gauge Aluminum coated Mylar, a possible material to be used for the proposed gossamer space structure, is used as the baseline material for this study. Thickness and density of this material are $19 \mu\text{m}$ and 1.40g/cm^3 , respectively. The mass contribution of the ribs is neglected here. To eliminate area dependence in the calculations, the differential pressure is calculated as follows

$$\delta P_{g,\text{radial}} = \frac{\delta F_{g,\text{radial}}}{A} \approx \rho t \frac{3\mu}{r_c^3} d \quad (12)$$

For the along-track configuration shown in Fig. 7(b) (large membrane area aligned with the velocity direction), the differential gravity force and pressure in the membrane normal direction are essentially zero

$$\delta F_{g,\text{along-track}} \approx \delta P_{g,\text{along-track}} \approx 0 \quad (13)$$

In the orbit normal configuration in Fig. 7(c) (large membrane area facing the direction of the angular momentum vector), differential gravity will tend to compress the structure. The free-body diagram of this setup is shown in Fig. 4(b). The linearized differential gravity force in this configuration is given by Eq. (14) [28].

$$\delta F_{g,\text{normal}} \approx -m \frac{\mu}{r_c^3} d \quad (14)$$

Similarly, the differential gravity pressure is

$$\delta P_{g,\text{normal}} = \frac{\delta F_{g,\text{normal}}}{A} \approx -\rho t \frac{\mu}{r_c^3} d \quad (15)$$

The equation for the disturbance force from solar radiation pressure is given by [35]:

$$P_{\text{SRP}} = \frac{F_{\text{SRP}}}{A} = p_{\text{SR}} c_R \quad (16)$$

where

$$p_{\text{SR}} = 4.57e^{-6} \text{N/m}^2 \quad (17)$$

is the nominal solar pressure at 1 AU from the sun, c_R is the reflectivity, and A is the area exposed to the sun. Note that the solar radiation pressure is independent of separation distance, area and orbit altitude. This pressure will therefore be identical at LEO and GEO orbits. It is assumed here that one membrane is fixed and the other membrane

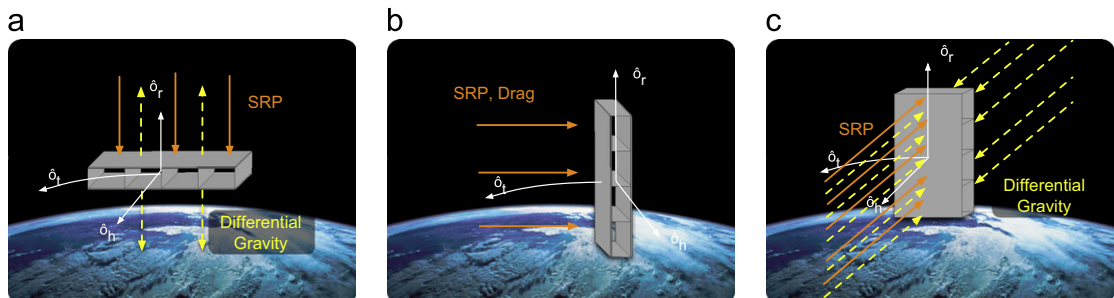


Fig. 7. Possible orbital configurations of the membrane sandwich structure with worst-case compressive orbital perturbations illustrated. (a) Radial configuration. (b) Along track configuration. (c) Orbit normal configuration.

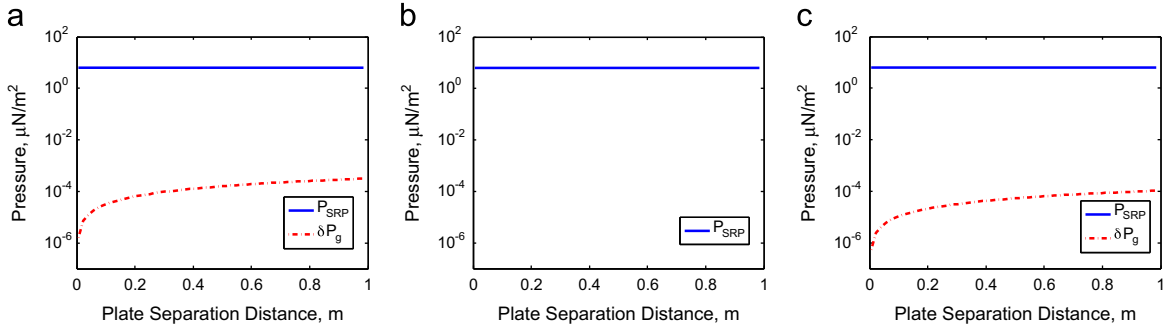


Fig. 8. Magnitudes of disturbance pressures in the radial, along-track, and normal configurations at GEO, mass $m=0.01$ kg. (a) Radial configuration. (b) Along track configuration. (c) Orbit normal configuration.

is experiencing pressure from solar radiation across the entire membrane surface. This is an assumption to provide a worst-case scenario of compression and not to describe the structural design.

These GEO perturbations force magnitudes are next compared for the three configurations illustrated in Fig. 7.

5.1.1. GEO orbit radial configuration

The orbit radial configuration is defined as the large areas of each membrane to be nadir facing, as shown in Fig. 7(a). Considering a worst case scenario, the solar radiation pressure would act directly normal to one plate. To avoid compression of the membrane structure, the inflationary electrostatic pressure must be greater than this differential solar radiation pressure. Fig. 8(a) shows a comparison of the magnitudes of disturbing pressures experienced at GEO for the sandwich structure.

Fig. 8(a) illustrates that the differential gravity forces are several orders of magnitude smaller than the solar radiation pressure. This result differs from the perturbation analysis for Coulomb formation flying or tethered Coulomb structures in which the differential gravity has a much larger effect. The cause for this difference is that both separation distances and masses are orders of magnitude smaller for the gossamer 2-membrane rib structure. The much larger area to mass ratio causes the solar radiation pressure to dominate. As a result the tensioning effect of the radial differential gravity term provides negligible relief on the overall inflationary force requirement.

5.1.2. GEO along-track configuration

In the along-track configuration, differential gravity has no effect on the sandwich structure. The only disturbance force is therefore solar radiation pressure, and the separation distance of the membranes will have no effect on the required electrostatic force for inflation. Again assuming a worst case alignment of the incident sun light with respect to the outer membrane surface, the resulting compressive solar radiation pressures are shown in Fig. 8(b). Because this differential solar radiation pressure model is independent of the membrane separation distance, the minimum required inflationary pressure is a fixed value regardless of the sandwich structure thickness.

5.1.3. GEO orbit normal configuration

Fig. 8(c) shows a comparison of the magnitudes of disturbing pressures experienced at GEO for an inflated sandwich structure in the orbit normal configuration. These magnitudes are nearly identical to the radial configuration, with the exception that in the normal configuration, differential gravity tends to compress the structure instead of providing tension, as in the radial configuration. Again the solar pressure dominates the required inflationary force for this GEO configuration.

5.2. Perturbations in LEO

Next, let us consider a membrane structure which is flying at LEO altitudes. In addition to the differential gravity pressures and solar radiation pressure expressed in Eqs. (12), (15), and (16), the perturbation from atmospheric drag is also considered. The drag force at these altitudes cannot be neglected as a perturbation as it may be at GEO altitudes. The force on the leading plate is calculated with [35]:

$$F_D = -\frac{1}{2} C_D A \rho v_{rel}^2 \frac{\mathbf{v}_{rel}}{|\mathbf{v}_{rel}|} \quad (18)$$

Again, to eliminate area dependence, the differential pressure from drag is calculated with:

$$P_D = -\frac{1}{2} C_D \rho v_{rel}^2 \frac{\mathbf{v}_{rel}}{|\mathbf{v}_{rel}|} \quad (19)$$

This force, however, is only considered for the along-track configuration. Here the large area of one plate is bombarded by the rarified atmospheric particles, while the other plate is protected in the wake of the leading plate. The resulting differential drag force on the leading plate tends to compress the structure. In the orbit radial and normal configurations the differential drag forces are negligible as no significant area is presented relative to the incoming rarified atmosphere. For the 2 membrane structure with an area of 0.5 m^2 and a mass of 0.01 kg , a study is performed to determine the altitude at which the drag force diminishes versus the differential solar radiation forces. Values for atmospheric density are calculated using the MSIS-E-90 Atmospheric Model.

As shown in Fig. 9, below approximately 500 km the atmospheric drag pressure is the dominating perturbation.

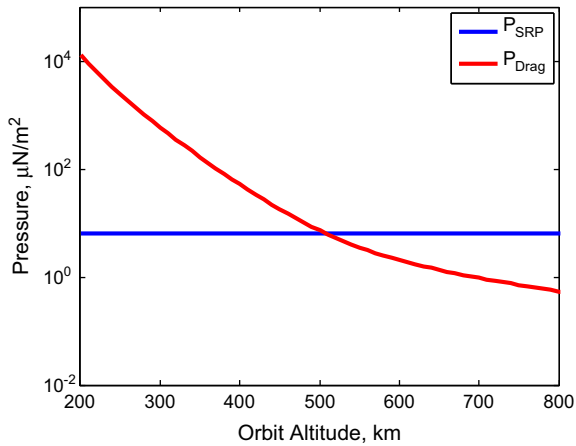


Fig. 9. Disturbance pressure magnitude as a function of altitude in LEO.

Above this altitude, the density becomes too low to have an appreciable effect. Near and below this altitude, the required charge densities and corresponding potentials to inflate a membrane structure must take the differential atmospheric drag into careful consideration. At low altitudes, large area EIMS yield large atmospheric drag forces, thus making it viable as a deployable drag de-orbiting device.

6. Minimum electric potentials to offset perturbations

Electrostatic inflation of a structure occurs when an electrostatic potential is applied and the charges distributed on the outer surface repel each other, expanding the structure. The potentials must be high enough to produce sufficiently large electrostatic forces for self-repulsion to negate the compressive differential forces from gravity, solar radiation pressure, and atmospheric drag that would be experienced in orbit. In Ref. [7], the required charge densities to produce these repulsive pressures between membranes of simple electrostatically inflated structures to avoid compression of the structure in the normal direction due to orbital perturbations after deployment are discussed. Voltage, however, is the quantity which will be actively controlled in the space environment to inflate the structure, therefore it must be determined from these required charge densities. As the structures are not shapes with simple capacitance relationships, such as a sphere, a relationship between the potential and charge is not analytically known. In the following section, the procedure for determining the voltage required for producing sufficient electrostatic inflation pressure to offset orbital perturbation pressures for a membrane sandwich structure with a numerical electrostatic field solver is discussed.

6.1. Charge density requirements

In the previous section, the magnitudes of disturbance pressures from differential gravity, solar radiation pressure and atmospheric drag are discussed for different orbit regimes and configurations of the membrane sandwich

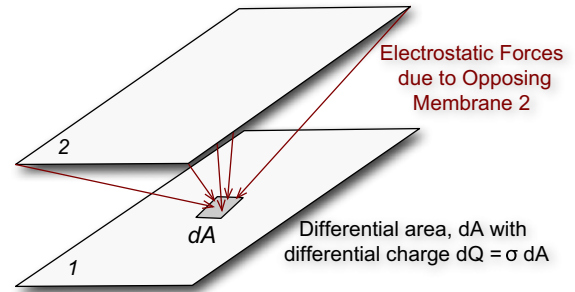


Fig. 10. Differential area element experiencing electrostatic forces from the distributed charge on the opposing membrane.

structure. For inflation of the structure, there must be sufficient electrostatic pressure across the entire surface of the membrane to offset these perturbations. This required pressure to exactly offset the disturbances will be associated with a required electrostatic charge density which is referred to as the minimum charge density on the membrane. Below this minimum charge density, the structure could compress or collapse.

Consider the two membrane setup shown in Fig. 10. We desire to find the required charge density on a small element of area dA such that the electrostatic pressure is at least the magnitude of the normal disturbance pressure. The charge on this differential area is:

$$dq = \sigma dA \quad (20)$$

The fundamental electrostatic force equation yields the differential force on this area due to the electric field normal to the surface:

$$dF = E_n dq \quad (21)$$

Rewriting this equation as the pressure and substituting Eq. (20) yields:

$$dP = \frac{dF}{dA} = \frac{E_n \sigma dA}{dA} = \sigma E_n \quad (22)$$

Application of Gauss's Law yields the electrostatic field at the surface of the membrane with knowledge of the local charge density;

$$E_n = \frac{\sigma}{\epsilon_0} \quad (23)$$

The pressure on the small area element is therefore only a function of the charge density on the membrane:

$$dP = \frac{\sigma^2}{\epsilon_0} \quad (24)$$

Eq. (24) can thus be rearranged to solve for the minimum charge density at any location on the membrane to create a required inflationary pressure level (P_{req}):

$$\sigma = \sqrt{\epsilon_0 P_{req}} \quad (25)$$

This paper is concerned with the compressive pressures of membrane-normal orbital perturbations. The relationship between the required electrostatic forces and these disturbance forces is expressed in Eqs. (2) and (3). The required pressure expressions are thus obtained for one or

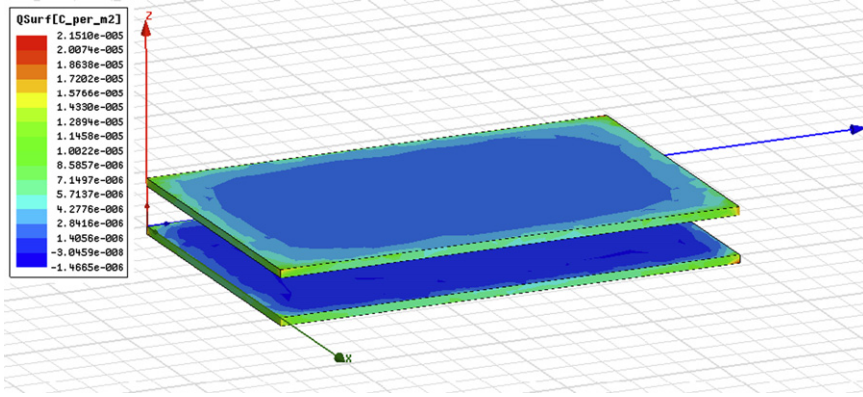


Fig. 11. Numerical solutions of surface charge distribution on two charged plates.

two sided disturbances, respectively:

$$P_{req} = \frac{P_{SRP} + P_D}{2} \tag{26a}$$

$$P_{req} = P_g \tag{26b}$$

All disturbance pressures (here, Eqs. (26a) and (26b)) are added and subsequently used in Eq. (25) to determine approximate minimum required charge densities at GEO and LEO.

6.2. Non-uniformity of the charge distribution

When considering the minimum required charge density, it is important to consider the non-uniformity of the charge distribution on the membranes. Maxwell 3D, a 3D electrostatic solver software has been used to aid in understanding the true charge distributions. Numerical results show that surface charge is highest at corners, as can be seen in Fig. 11, where red represents the largest value of surface charge. As seen in Fig. 11, the minimum charge density is in the center of the membrane. From Eq. (25), this will also be the location of minimum electrostatic pressure.

6.3. Geometric considerations for two plate configuration

A simple analytical capacitance relationship between the required charge densities (as described thus far) and the required voltage does not exist. Numerical electrostatic field modeling is therefore required to determine the capacitance of the system. In this section, the effect of geometry on the capacitance relationship is studied to better understand which configurations are preferable for electrostatic inflation.

To understand the capacitance relationship for the sandwich configuration, Ansoft’s Maxwell 3D software [36] was used to create geometries, simulate electrostatic fields, and numerically determine forces on the membranes. The numerical simulations were performed for a model of two conducting, finite plates in a vacuum. For the two plate configuration, the matrix relationship is as shown in Eq. (27), where V is the voltage and Q is the total charge on the membrane. The diagonal components of this symmetric

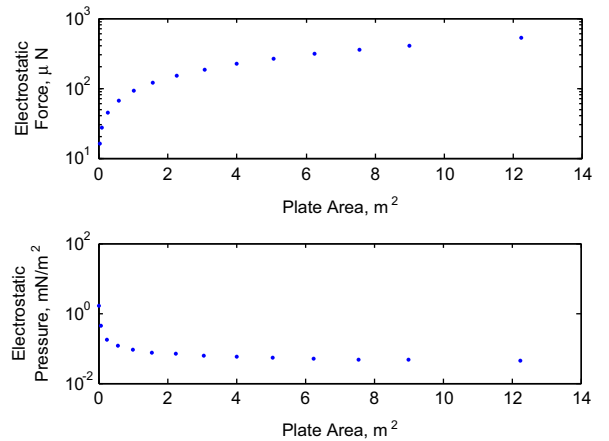


Fig. 12. Numerical simulation of effect of varying structure area on the system, fixed separation 2 cm, fixed potential 1 kV.

matrix are the capacity coefficients and the off-diagonal terms are the electrostatic induction coefficients [37]. The induction coefficients are negative values and account for the decrease in the potential due to a nearby conductor.

$$\begin{bmatrix} Q_1 \\ Q_2 \end{bmatrix} = \begin{bmatrix} C_{11} & C_{12} \\ C_{21} & C_{22} \end{bmatrix} \begin{bmatrix} V_1 \\ V_2 \end{bmatrix} \tag{27}$$

The values of the capacitance matrix are dependent only on the geometry of the conductors. For this system, the capacitance can be altered by changing the area of the plates or by changing the separation distance between the plates. Fig. 12 illustrates the effect of changing the area of the structure. Increasing the area increases the capacitance of the system, allowing more charge to reside on the structure for a fixed value of potential. The repulsive forces between the two membranes therefore increase with this additional charge, as shown in the top plot of Fig. 12. When the pressure is considered, however, the increase in area causes a decrease in electrostatic pressure. Pressure is the quantity in which we are most interested, not total force, as the distributed pressures of orbital perturbations must be offset across the whole area of the structure. This suggests that electrostatic inflation can be achieved more easily for

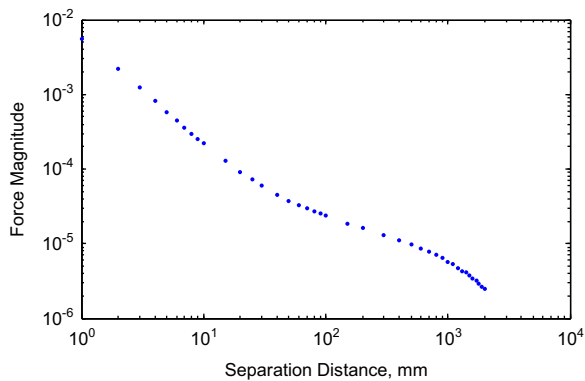


Fig. 13. Numerical simulation of effects of varying separation distance between membranes on electrostatic force; fixed area of 1 m^2 , fixed potential 1 kV .

small area structures. The effect of changing the area on the system capacitance diminishes as the areas become larger than a few square meters, and the effect of area change on electrostatic pressure has nearly settled by areas of 4 m^2 .

The effect of varying the separation distance on the system capacitance is very significant. Fig. 13 illustrates the trends for a range of separation distances between membranes with a fixed potential and area. The electrostatic forces become larger as the two membranes are brought closer per Coulomb's law and because the system capacitance increases as two conducting bodies become closer. This result suggests that it will be most advantageous to have the two membranes very close. Small separation distances between membranes are also preferred when considering Debye Shielding, especially at LEO where Debye lengths can be close to the order of the separation distances considered here.

6.4. Voltage requirements for inflation

To explore the results thus far presented, an example of the required voltage for a two-membrane electrostatically inflated structure with 1 m^2 area in the along-track configuration of a GEO orbit is considered. To summarize the procedure, first the normal orbital perturbations are determined. Using Eq. (25), the determined perturbations yield the required charge density to maintain inflation. Maxwell 3D is then used to draw appropriate geometries, solve the full electrostatic field solution, and determine the voltage which will yield the required minimum charge density.

For the given orbit and configuration, the potentials necessary to offset perturbing orbital pressures are shown in Fig. 14 for a range of membrane separation distances. From Fig. 14 it can be seen that the required potential is only on the order of a few hundred volts. This is a very small voltage compared to the kilovolt levels that have been achieved through active charging in GEO. Even natural charging levels at GEO during eclipse can far exceed this level.

The relationship between voltage and minimum charge density is shown in Fig. 15 for two membranes with areas of 1 m^2 at a fixed separation distance of 20 mm . This plot illustrates how voltage requirements scale as the orbital

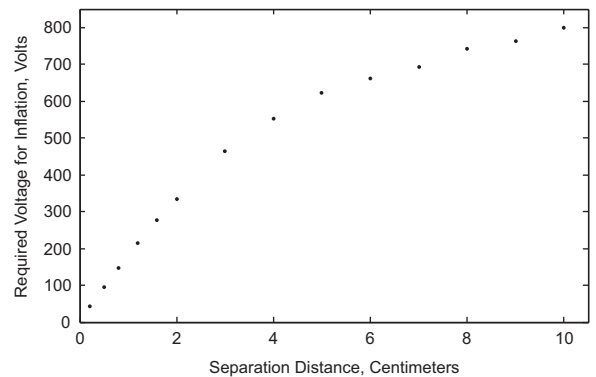


Fig. 14. Required voltage for offset of compressive orbital perturbations at GEO of a sandwich structure for a range of separation distances; area = 1 m^2 .

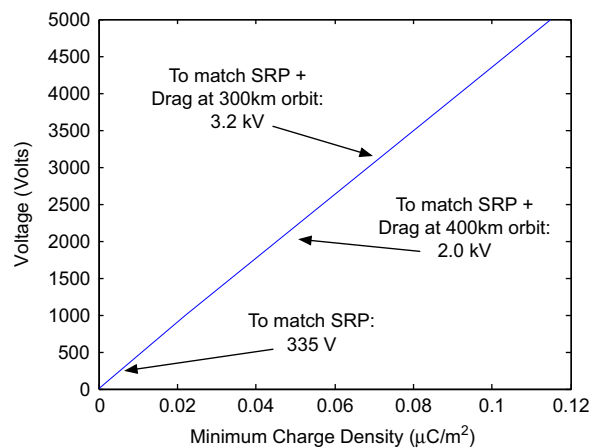


Fig. 15. Numerical evaluation of the relationship between voltage applied to the membranes and the minimum value of charge density, shown with $A = 1 \text{ m}^2$ and $d = 20 \text{ mm}$.

perturbation pressures increase from GEO to different LEO altitudes. Fig. 15 shows that the relationship between these two parameters appears linear over the domain of voltages investigated. As the drag increases in lower LEO orbits, the required voltages to offset this pressure remains in the few kilovolt range, which remains below the previously achieved on-orbit charging levels.

It should be noted that the voltage that would be used to inflate the structure would be greater than just this equilibrium voltage. These results reflect a minimum that would be necessary to exactly offset orbital perturbations, but not provide any stiffness beyond this. Additional charging would be required to provide more stiffness, which would be especially desirable during attitude maneuvers which may deform the structure. The procedure described in this paper will also be applicable to determine the voltages to offset the pressures encountered during attitude maneuvers. What is important here is that this analysis provides a good estimate of the order of magnitude of required potentials for maintaining inflation and these required potentials are feasible for charging in a LEO or GEO environment.

7. Conclusion

The focus of this paper is the introduction of an electrostatic inflation method and a study of the required absolute potentials of space-based layered membrane structures to counteract membrane-normal compressive pressures from orbital perturbations. Potentials on the membrane structures must be high enough to produce sufficient electrostatic pressures to counteract the differential pressures from gravity, solar radiation, and drag that would be experienced in orbit. In the geostationary orbit regime, the differential solar radiation pressure is the dominant perturbation. In low Earth orbit, atmospheric drag becomes dominant below approximately 500 km. Determination of differential orbital pressures allows for the calculation of the required charge densities for inflation. To determine the corresponding voltage requirements assuming the electrostatically inflated membrane structure is to maintain shape while experiencing orbital perturbations, 3D electrostatic solver software was used to numerically determine the electrostatic field solution. For a $1 \times 1 \text{ m}^2$ structure in geostationary orbit, it was found that only hundreds of volts are needed to offset orbital perturbations. Active and even passive charging in geostationary orbits have far exceeded this number on several spacecraft. In LEO, potentials on the order of a few kilovolts are required. These determined potentials serve as a minimum to only offset disturbance pressures and larger values would be desirable to provide additional stiffness to the structure, especially during attitude maneuvers. Even these minimum values, however, are orders of magnitude smaller than what has been achieved on previous missions. Selected future work includes studying required pressures for attitude maneuvers, incorporating Debye shielding in LEO, and investigating structural deformations such as pillowing and wrinkling.

References

- [1] R.E. Freeland, G.D. Bilyeu, G.R. Veal, M.M. Mikulas, Inflatable deployable space structures technology summary, in: 49th International Astronautical Congress, Melbourne, Australia, 1998.
- [2] R.E. Freeland, G.D. Bilyeu, G.R. Veal, M.D. Steiner, D.E. Carson, Large inflatable deployable antenna flight experiment results, *Acta Astronaut.* 41 (1997) 267–277.
- [3] J.A. Banik, T.W. Murphy, Synchronous deployed solar sail subsystem design concept, in: AIAA-2007-1837, 47th AIAA Structures, Dynamics, and Mechanics of Materials Conference, 2007.
- [4] D.P. Cadogan, J.K. Lin, M.S. Grahne, Inflatable solar array technology, in: AIAA-99-1075, 37th AIAA Aerospace Sciences Meeting and Exhibit, 1009.
- [5] D.P. Cadogan, J. Stein, M.S. Grahne, Inflatable composite habitat structures for lunar and mars exploration, *Acta Astronaut.* 44 (1999) 399–406.
- [6] C.H.M. Jenkins (Ed.), Gossamer Spacecraft: Membrane and Inflatable Structures Technology for Space Applications, Progress in Astronautics and Aeronautics, vol. 191, American Institute of Aeronautics and Astronautics, 2001.
- [7] L.A. Stiles, H. Schaub, K.K. Maute, J. Daniel F. Moorer, Electrostatic inflation of membrane space structures, in: AAS/AIAA Astro-dynamics Specialist Conference, Toronto, Canada, 2010.
- [8] L.A. Stiles, H. Schaub, K.K. Maute, Voltage Requirements for Electrostatic Inflation of Gossamer Space Structures, AIAA Gossamer Systems Forum, Denver, CO, 2011.
- [9] R.K. Tripathi, J.W. Wilson, R.C. Youngquist, Electrostatic space radiation shielding, *Adv. Space Res.* 42 (2008) 1043–1049.
- [10] J.H. Cover, W. Knauer, H.A. Maurer, Lightweight reflecting structures utilizing electrostatic inflation, US Patent 3,546,706, 1966.
- [11] H.A. MacEwen (Ed.), Stretched Membrane with Electrostatic Curvature (SMEC) Mirrors, vol. 4849, SPIE, 2002.
- [12] L.B. King, G.G. Parker, S. Deshmukh, J.-H. Chong, Spacecraft Formation-Flying using Inter-Vehicle Coulomb Forces, Technical Report, NASA/NIAC, 2002.
- [13] H. Schaub, G.G. Parker, L.B. King, Challenges and prospect of Coulomb formations, *J. Astronaut. Sci.* 52 (2004) 169–193.
- [14] J. Berryman, H. Schaub, Analytical charge analysis for 2- and 3-craft Coulomb formations, *AIAA J. Guidance Control Dyn.* 30 (2007) 1701–1710.
- [15] H. Schaub, C. Hall, J. Berryman, Necessary conditions for circularly-restricted static Coulomb formations, *J. Astronaut. Sci.* 54 (2006) 525–541.
- [16] A. Natarajan, H. Schaub, Linear dynamics and stability analysis of a Coulomb tether formation, *AIAA J. Guidance Control Dyn.* 29 (2006) 831–839.
- [17] S. Wang, H. Schaub, Switched Lyapunov function based Coulomb control of a triangular 3-vehicle cluster, in: AAS/AIAA Astrodynamics Specialist Conference, Pittsburgh, PA, 2009.
- [18] C.R. Seubert, H. Schaub, Tethered Coulomb structures: prospects and challenges, *J. Astronaut. Sci.* 57 (2009) 347–368.
- [19] C.R. Seubert, S. Panosian, H. Schaub, Dynamic feasibility study of a tethered Coulomb structure, in: AAS/AIAA Astrodynamics Specialist Conference, Toronto, Canada. AIAA-2010-8131, 2010.
- [20] D.A. McPherson, D.P. Cauffman, W. Schober, Spacecraft charging at high altitudes—the scatha satellite program, in: AIAA Aerospace Sciences Meeting, Pasadena, CA, 1975.
- [21] E.G. Mullen, M.S. Gussenhoven, D.A. Hardy, T.A. Aggson, B.G. Ledley, Scatha survey of high-voltage spacecraft charging in sunlight, *J. Geophys. Sci.* 91 (1986) 1474–1490.
- [22] R.C. Olsen, Record charging events from applied technology satellite 6, *J. Spacecr. Rockets* 24 (1986) 362–366.
- [23] I. Katz, Structure of the bipolar plasma sheath generated by SPEAR I, *J. Geophys. Res.* 94 (1989) 1450–1458.
- [24] L.B. King, G.G. Parker, S. Deshmukh, J.-H. Chong, Study of inter-spacecraft Coulomb forces and implications for formation flying, *AIAA J. Propul. Power* 19 (2003) 497–505.
- [25] J.A. Bittencourt, *Fundamentals of Plasma Physics*, third ed. Springer, 2004.
- [26] N. Murdoch, D. Izzo, C. Bombardelli, I. Carnelli, A. Hilgers, D. Rodgers, Electrostatic tractor for near earth object deflection, in: 59th International Astronautical Congress, Glasgow, Scotland. Paper IAC-08-A3.1.5, 2008.
- [27] D.E. Hastings, H.B. Garrett, *Spacecraft–Environment Interactions*, Cambridge University Press, 1996.
- [28] C.R. Seubert, H. Schaub, Tethered Coulomb structures: prospects and challenges, in: AAS F. Landis Markley Astrodynamics Symposium, Cambridge, MA. Paper AAS 08–269, 2008.
- [29] L.A. Stiles, C.R. Seubert, Effective Coulomb force modeling in a space environment, in: AAS/AIAA Astrodynamics Specialist Conference, Charleston, SC, 2012.
- [30] V. Pierrard, J. Goldstein, N. André, V. Jordanova, G. Kotova, J. Lemaire, M. Liemohn, H. Matsui, Recent progress in physics-based models of the plasmasphere, *Space Sci. Rev.* 145 (2009) 193–229.
- [31] M.F. Thomsen, M.H. Denton, B. Lavraud, M. Bodeau, Statistics of plasma fluxes at geosynchronous orbit over more than a full solar cycle, *Space Weather* 5 (2007).
- [32] H.B. Garrett, S.E. DeForest, An analytical simulation of the geosynchronous plasma environment, *Planet. Space Sci.* 27 (1979) 1101–1109.
- [33] W. Lennartsson, D.L. Reasoner, Low-energy plasma observations at synchronous orbit, *J. Geophys. Res.* 83 (1978) 2145–2156.
- [34] J.L. Herr, M.B. McCollum, Spacecraft Environments Interactions: Protecting Against the Effects of Spacecraft Charging, Reference Publication 1354, NASA Marshall Space Flight Center, 1994.
- [35] D.A. Vallado, *Fundamentals of Astrodynamics and Applications*, Space Technology Library, third ed. Springer, 2007.
- [36] *User's Guide: Maxwell 3D*, Ansoft, 11 edition, 2010.
- [37] L.D. Landau, E.M. Lifshitz, *Electrodynamics of Continuous Media*, Course of Theoretical Physics, vol. 8, Addison-Wesley Publishing Company, Inc., 1960.